Capacitance properties of graphite/polypyrrole composite electrode prepared by chemical polymerization of pyrrole on graphite fiber

Jong Hyeok Park[a], Jang Myoun Ko[b], O. Ok Park[a,*], Dong-Wen Kim[b]

[a]*Department of Chemical Engineering, Center for Advanced Functional Polymer (CAF Poly), Korea Advanced Institute of Science and Technology, 373-1 Kusong-dong, Yusung-Gu, Taejon 305-701, South Korea*
[b]*Department of Chemical Technology, Hanbat National University, San 16-1, Dukmyung-Dong, Yusung-Gu, Taejon 305-719, South Korea*

Abstract

Composite electrodes for supercapacitors are prepared via chemical polymerization of pyrrole (Py) on the surface of a porous graphite fiber matrix. The capacitance properties are investigated with cyclic voltammetry (CV), ac impedance spectroscopy and charge–discharge tests. These electrodes show a specific capacitance of about $400 \, \text{F} \, \text{g}^{-1}$ and a Coulombic efficiency of 96–99%. This indicates that the dipping method is quite suitable for the modification of carbon-based porous graphite fiber to improve the performance of electrodes which can be used in supercapacitors. © 2002 Elsevier Science B.V. All rights reserved.

1. Introduction

Supercapacitors are being considered for a variety of applications not only in electric vehicles and uninterruptible power supplies but also in memory protection of computer electronics and cellular communication devices [1–3].

Two types of supercapacitor are under development. One is the electric double-layer capacitor, and the other is the redox capacitor. In the former, energy storage arises mainly from the separation of electronic and ionic charges at the interface between electrode materials with high-specific area (such as carbon) and the electrolyte solution. In the latter, fast Faradaic reactions take place at the electrode materials at characteristic potentials, as in batteries. While activated carbon has demonstrated a higher cycle-life, its capacitance value and electrical conductivity are lower than those of conducting polymer. On the other hand, electrically conducting polymers including polypyrrole (PPy), polyaniline, etc. have been found to have higher capacitance because capacitive and Faradaic currents contribute to the charge storage. The conducting polymers, however, have disadvantages that include a lower cycle-life in charge–discharge duty than carbon-based electrodes because the redox sites in the polymer backbone are not sufficiently stable for many repeated redox processes.

Some methods have been attempted to improve the capacitance and the conductivity of carbon-based supercapacitors. For example, fabrication of a conducting polymer/graphite fiber composite with PPy have been successfully made by using electrochemical polymerization of pyrrole (Py) on the surface of graphite fiber and show higher capacitance and conductivity [4,5]. The, electrochemical method has two disadvantages, however, compared with the method of chemical polymerization. One is that the electrochemical method is limited in terms of the mass production of composite electrodes. The other disadvantage is that the electrochemical method is not suitable for preparing controlled polymer films with thicknesses above 100 µm although it is suitable for preparing very thin films of polymer. If thin polymer film with a very high-specific capacitance per unit mass is converted to specific capacitance per unit area, this value is less than that for a carbon-based supercapacitor because of the small deposited polymer mass.

In the present study, PPy/graphite composite electrodes are chemically fabricated by using sequential dipping methods in order to overcome problems encountered with the electrochemical composite method. Since we are interested in the application of composites as active electrode materials in electrochemical supercapacitors, their relevant electrochemical properties are investigated by means of cyclic voltammetry (CV), electrochemical impedance spectroscopy (EIS), and charge–discharge tests.

* Corresponding author. Tel.: +82-42-869-3923; fax: +82-42-869-3910.
E-mail address: oopark@kaist.ac.kr (O.O. Park).

2. Experimental

Py (99%) was purchased from Aldrich and then distilled before use. $Fe(NO_3)_3 \cdot 9H_2O$ was purchased from Daejung and analytical grade pure methanol (MeOH, Merck), and dichloromethane (Aldrich) were used after distillation. KCl (Aldrich) was used as a supporting salt in the electrochemical examination.

PPy/graphite composite electrodes were fabricated using a commercially available porous graphite substrate (Toray Inc.). This material has a high porosity of the order of 75%, and a bulk density of $\sim$0.45 g cm^{-3}. The electrical resistivity of the graphite fiber is less than 0.07 Ω cm so that the fiber network provides an electronically conductive skeletal current-collector for the electroactive polymer.

Chemically oxidative polymerization of Py on the surface of the graphite fiber was performed by using an alternate immersion of the substrate into the solution with Py and into the solution with oxidant. The detail operating conditions for one cycle of polymer deposition are summarized in Table 1. The synthesis was carried out in a glove box flushed with nitrogen gas. The film thickness was controlled by the deposition cycles.

FT-IR spectroscopy (Bomem MB 102) was used to identify the chemical structure of the prepared PPy/graphite composite electrode. The infrared spectrum of the PPy samples utilized in this study was compared with that reported in the literature, and the PPy/graphite composite was observed with scanning electron microscopy (SEM, Philips 535).

All electrochemical half-cell measurements were conducted in a three-electrode cell which consisted of a three-neck 100 ml beaker equipped with a reference electrode (Ag/AgCl), a counter electrode (Pt), and a working electrode (PPy/graphite composite electrode). Measurements were carried out using a potentiostat/galvanostat (EG&G 263A). The apparent surface-area of cells was kept to about 4.0 cm^2. The charge capacitance was obtained from integration of the anodic or the cathodic waves in cyclic voltammograms between 0 and 0.8 V.

The capacitor cells were constructed with electrolyte-impregnated Cellgard 3501 sandwiched between two symmetrical PPy/graphite electrodes which were contacted with a current-collector (Pt foil). The electrodes were pre-wetted with electrolyte before use. The capacitor performance was characterized by means of impedance measurements and galvanostatic charge–discharge tests. The impedance measurements were carried out using a Solartron frequency response analyzer in the frequency range between 100 kHz and 10 mHz at a signal level of 0 mV. The charge–discharge performance of the capacitors was galvanostatically measured at different constant current densities for various cycles (Toyo Toscat 300U). The discharge capacitance C was evaluated from the linear part of the discharge curves using the following formula:

$$C = \frac{i\Delta t}{\Delta V} \tag{1}$$

where i is the constant current and Δt the time interval for the change in voltage ΔV. The Coulombic efficiency, η, was calculated using Eq. (2) with the same current used for charging and discharging, i.e.

$$\eta = \frac{t_D}{t_C} \times 100 \tag{2}$$

where t_D and t_C are the times for discharging the charging, respectively.

3. Results and discussion

The infrared spectra of the graphite fiber and PPy/graphite composite electrode obtained by the KBr method are shown in Fig. 1. All the PPy bands (conjugated double bond: 1560 cm^{-1}; amines: 1250 cm^{-1}, etc.) are present in the spectrum for the composite electrode [6].

The cyclic voltammograms obtained from PPy/graphite composite electrodes in 1 M KCl electrolyte, which were made with different dipping cycle times, are given in Fig. 2.
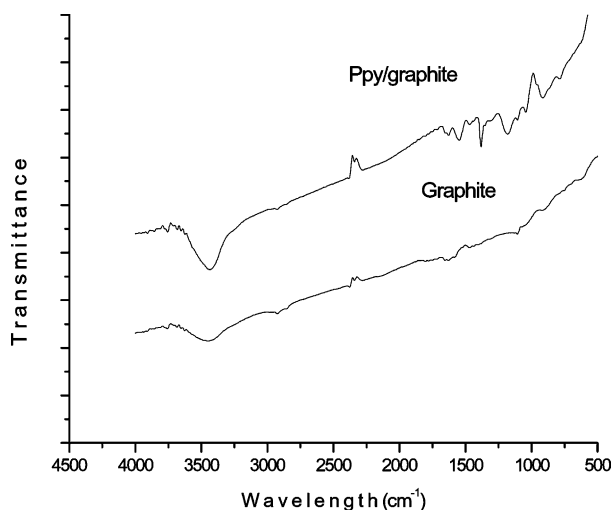
Table 1
Operating conditions for layer-by-layer preparation of PPy/graphite films

Step	Operation	Medium	Duration (s)
1	Immersion in monomer solution	Py 20 wt.% in CH$_2$Cl$_2$	4
2	Drying in glove box		300
3	Immersion in oxidizing solution	1 M oxidant in methanol	3
4	Polymerization		360
5–8	Subsequent rinsings	Methanol	60
9	Drying		600

Fig. 1. Infrared spectra of PPy/graphite fiber composite sample sintered with KBr.
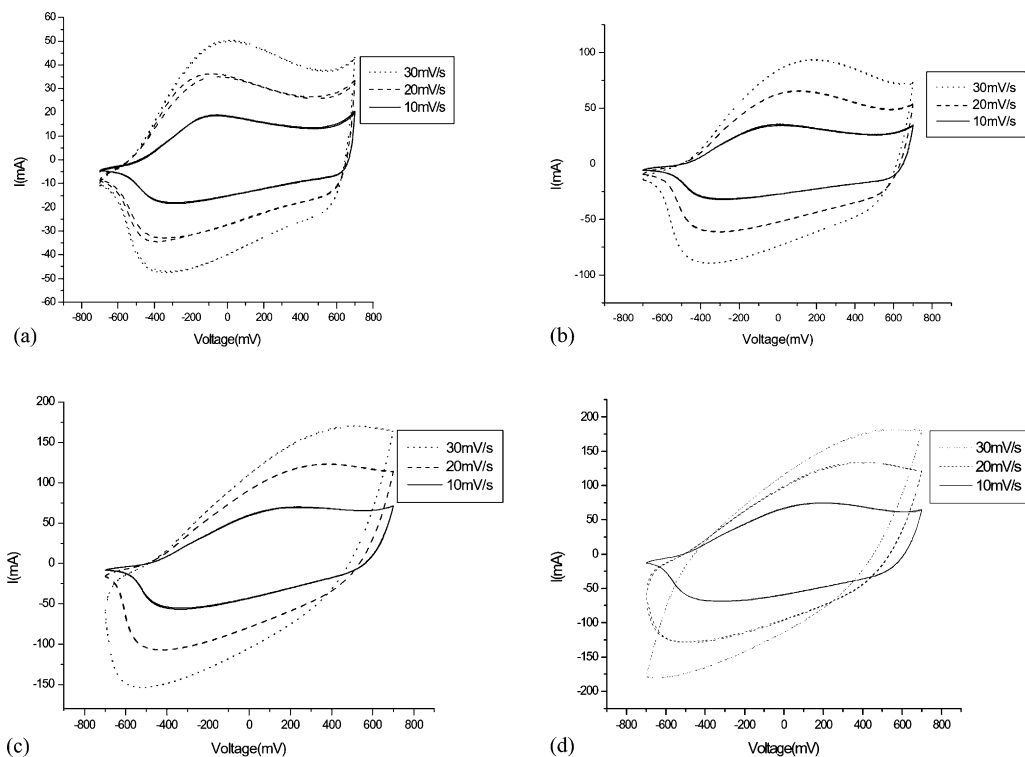
Fig. 2. Cyclic voltammograms of PPy/graphite fibre composite electrodes in 1 M KCl electrolyte. Electrodes prepared with dipping times at room temperature: (a) 1 cycle time; (b) 2 cycle time; (c) 3 cycle time; (d) 5 cycle time.

The electrodes deposited by two dipping cycle times, as shown in Fig. 2(a) and (b), show sharp oxidation and reduction current peaks at various sweep rates. On the other hand, the electrode deposited by five dipping cycle times (as shown in Fig. 2(d)) is characterized by broad peaks in contrast to the sharp peaks associated with thin films as shown in Fig. 2(a) and (b). This behavior is more marked with increasing sweep rate. To understand the above results, the surface areas of the pure graphite and PPy/graphite composite electrodes was determined to be less than $5\,m^2\,g^{-1}$ in both cases. The expected double-layer current for a capacitance is much less than the charge stored by the redox process of PPy itself. The total capacitance per unit area (at $10\,mV\,s^{-1}$) of the electrode increased monotonically with increasing dipping cycle times, but this behavior becomes saturated at four to five times, as shown in Fig. 3. Plots of the charge capacitance of the composite electrodes calculated from cyclic voltammograms as a function of sweep rate(s) are given in Fig. 4 to observe the influence of sweep rate on electrochemical performance. It is evident that the current response becomes increasingly influenced by the capacitive time constant (RC) of the sample at higher sweep rates. On increasing the sweep rate, the response is dominated by the RC time constant such that a capacitance region is not observed. The observed constant current charge–discharge behavior is plotted in Fig. 5.

To demonstrate the practical application of these composite electrodes, a capacitor configuration (type I) was fabricated and its charge–discharge properties were evaluated. A unit cell was constructed using the treated composite electrodes as both cathode and anode. The charge–discharge cycling curves of the pseudocapacitor using the composite electrode are presented in Fig. 5(a). Charge–discharge cycling was conducted between 0 and 1 V with a current density of $1\,mA\,cm^{-2}$ at room temperature. The charge–discharge curve showed linear behavior. The configuration
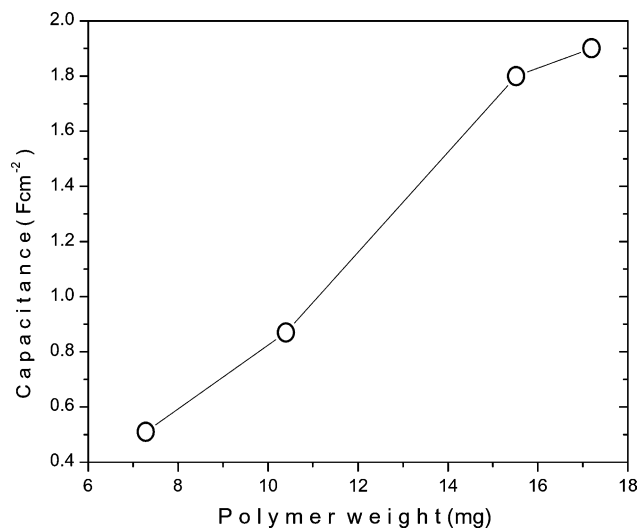

Fig. 3. Capacitance of PPy/graphite fibre composite electrode in 1 M KCl electrolyte at $10\,mV\,s^{-1}$ sweep rate.
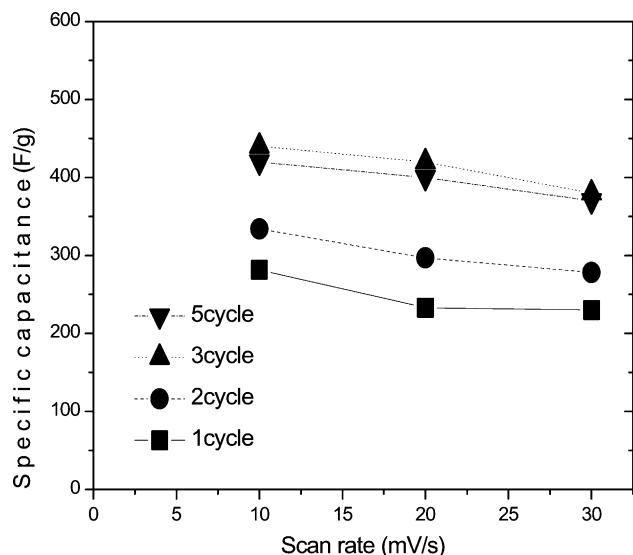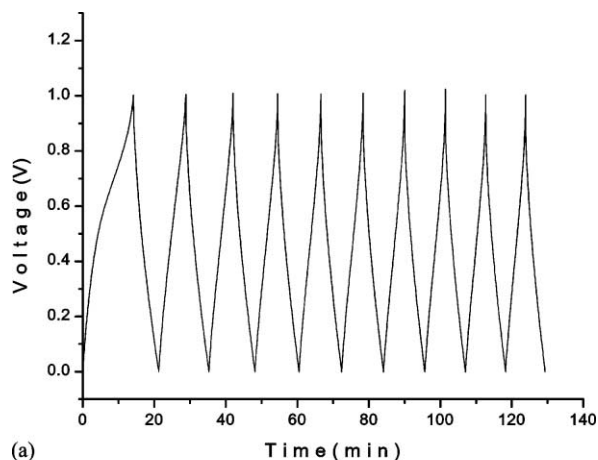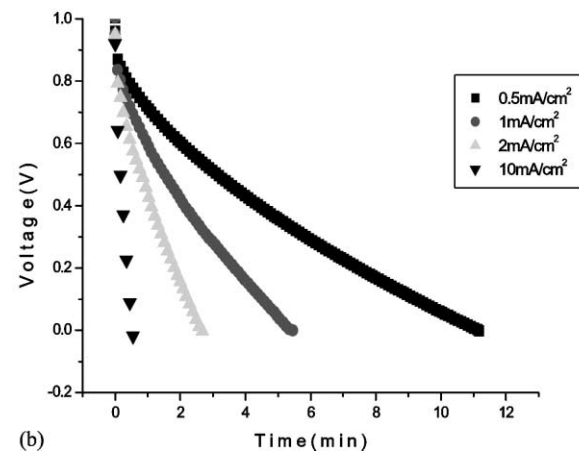
Fig. 4. Capacitance of PPy/graphite fibre composite electrode as a function of sweep rate for various deposited cycle times in 1 M KCl electrolyte.
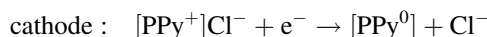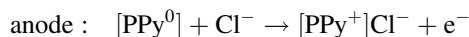

Fig. 5. (a) Charge–discharge curves for unit cell capacitor at 1 mA cm^{-2} current density; (b) discharge curves at various discharge current densities.

of these cells may be written as [PPy]/KCl/[PPy]. The reactions at the anode and cathode during discharge in a cell with 1 M KCl as an electrolyte can be written as

$$\text{anode}: \quad [\text{PPy}^0] + \text{Cl}^- \rightarrow [\text{PPy}^+]\text{Cl}^- + e^-$$

$$\text{cathode}: \quad [\text{PPy}^+]\text{Cl}^- + e^- \rightarrow [\text{PPy}^0] + \text{Cl}^-$$

For a fully-charged state of the cell, the anodic process is neutral because the PPy does not have any n-doping ability. The cathodic process is the fully-oxidized state and charge neutrality is maintained by the chloride ions. During the discharge process, the PPy in the cathodic process is reduced and the anode is oxidized to reach the same potential state. During discharge, the counter-ions ejected from the cathode are inserted in the anode electrode to maintain charge neutrality. The fall in cell voltage during discharge for a unit capacitor cell at various current densities is shown in Fig. 5(b). This behavior was recorded after 100 cycles. The resulted capacitance per unit mass calculated from the data in Fig. 5(b) is shown in Fig. 6 as a function of current density. The capacitance per unit mass decreases slightly with increasing current density.

Charge–discharge tests were also used to characterize the cycling behavior and kinetics of the PPy/graphite composite electrode. Several samples were examined for up to 100 cycles. The variation in discharge capacitance of a unit capacitor cell as a function of cycle number is given in Fig. 7. The capacitance is calculated at a current density of 1 mA cm^{-2} and no decrease in the capacitance is observed during 100 cycles. The Coulombic efficiency, η was calculated and is shown in Fig. 8 as a function of current density. The Coulombic efficiency of the capacitor over 1–100 cycles is between 96 and 99%.

EIS has been used extensively to study the redox processes of conducting polymers and to evaluate their ionic
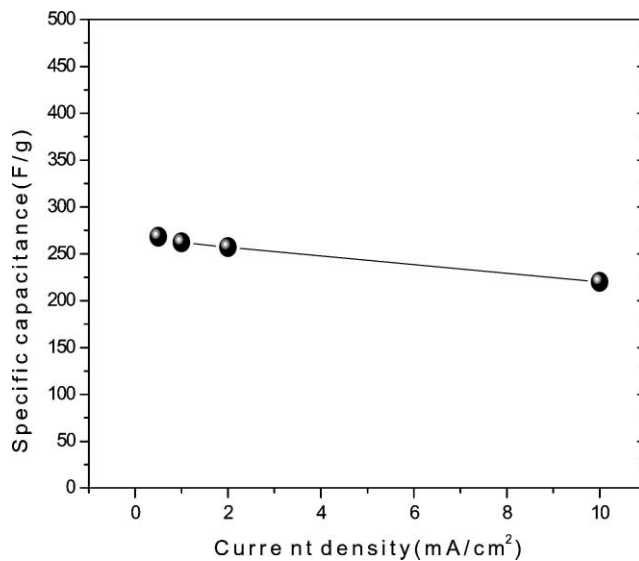

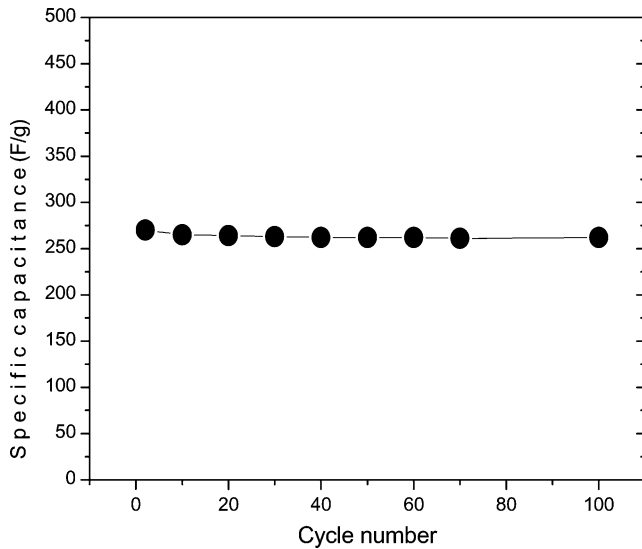Fig. 6. Discharge capacitance of unit cell as function of discharge current density.

Fig. 7. Variation of capacitance as a function of cycle number for unit cell capacitor at 1 mA cm^{-2} charge–discharge current density.

and electronic conductivities [4]. The impedance of a cell at a unit cell voltage of 0 V has been investigated to characterize the electrode in the doped state because both the anode and the cathode are in a partially doped state at 0 V [7]. It is expected that the impedance of the PPy films will follow the typical behavior. At high-frequency, a charge transfer-dominated regime is observed, while at lower frequencies, diffusion of charge in the polymer films dominates [8]. The frequency range of the diffusion behavior is controlled by the diffusion coefficient and film thickness. The high-frequency (real) impedance intercept of 0.7 Ω cm^{-2} in Fig. 9(a) reflects the resistance of the bulk electrolyte between the electrodes and the two working electrodes. The most important features of the impedance spectra in Fig. 9 are the resistance associated with
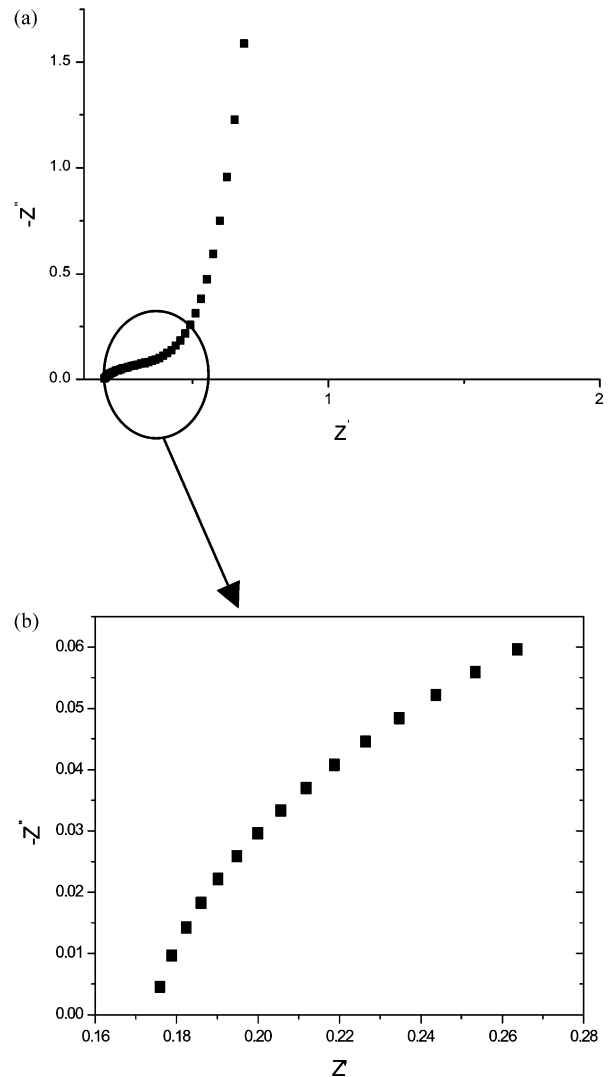

Fig. 9. Impedance spectrum of unit cell capacitor cell between 100 kHz and 10 mHz at 0 V signal level.
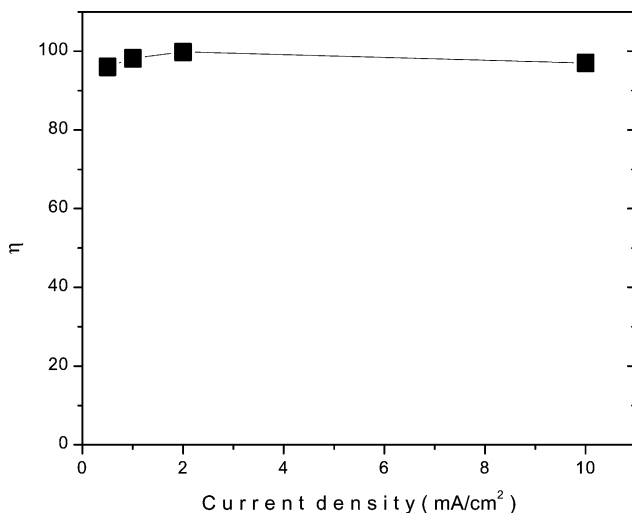
the transport process within the porous structure of the electrode. These resistance is evaluated from the difference in the real part of the impedance between low and high frequencies, and are seen from Fig. 9 to be about 2 Ω cm^{-2}

An electron micrograph of a plan view of the graphite fibre substrate is shown in Fig. 10(a). A typical example of the PPy/graphite composite electrode prepared by dipping method is presented in Fig. 10(b). The deposition cycle was two times and resulted in a mass of PPy of 10.04 mg per 4 cm^2. At low polymerization cycle numbers, where the porosity and contact surface-area of the composite electrodes are both high, ionic diffusion is fast in comparison with oxidation and reduction of the polymer. For higher dipping cycle numbers, however, the coated fibres begin to grow into each other which results in ionic diffusional resistance. This can be seen clearly in the electron micrograph shown in Fig. 10(c) and (d).

Fig. 8. Coulombic efficiency of charge–discharge for unit cell capacitor.
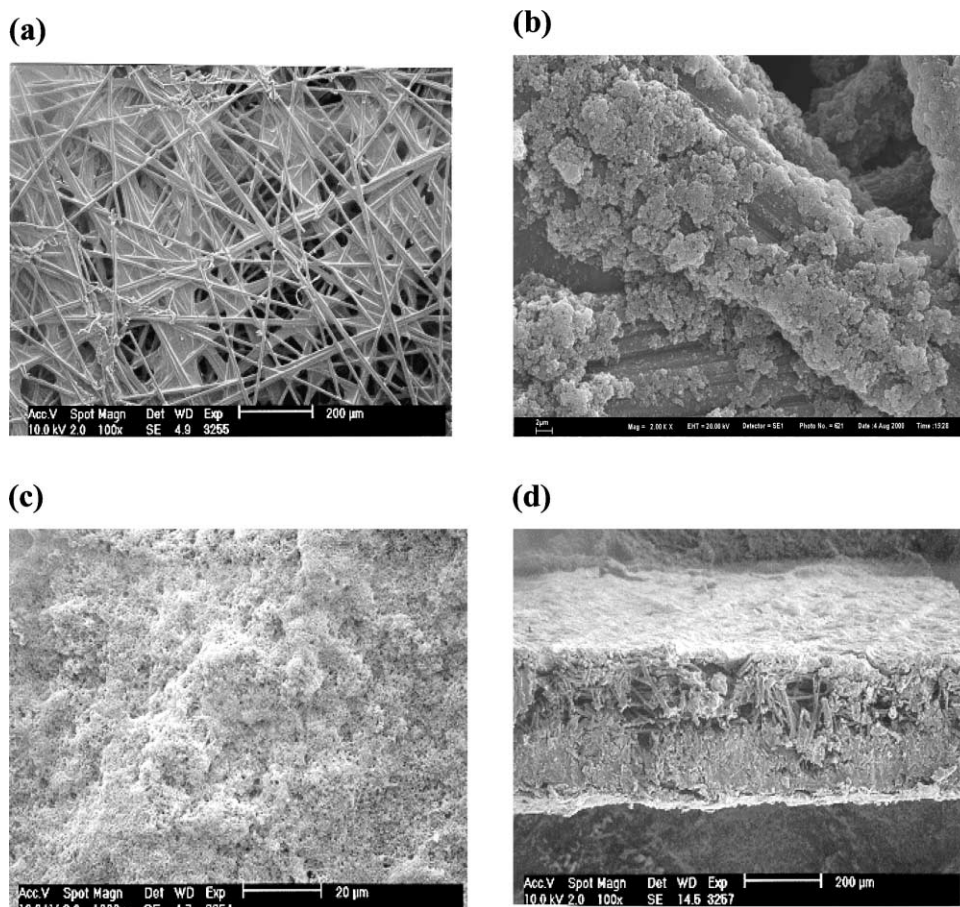
Fig. 10. (a) Scanning electron micrographs of plan view; (b) scanning electron micrograph of fibre plan view of morphology of PPy/graphite fibre composite electrode (two cycles); (c) scanning electron micrograph of plan view of morphology of PPy/graphite fibre composite electrode (10 cycles); (d) scanning electron microscopy of cross-section view of morphology of PPy/graphite fibre composite electrode (10 cycles).

4. Conclusions

A PPy-coated graphite composite prepared by the chemical dipping method has proved to be suitable for the manufacture of supercapacitor energy storage devices. The sequential dipping method provides a well coated, thickness-controlled PPy/graphite fiber composite electrode. The electrodes show a specific capacitance of $\sim$400 F g^{-1} and a Coulombic efficiency of 96–99%. This demonstrates that the dipping method is suitable for the preparation of a composite electrode for supercapacitors.

References

[1] B.E. Conway, W. Pell, Proceedings of the 8th International Seminar on Double-Layer Capacitors and Similar Energy Storage Devices, Florida Educational Seminars, Deerfield Beach, FL, 7–9 December, 1998.

[2] C Arbizzani, M. Mastragostino, B. Scosati, in: H.S. Nalwa (Ed.), Handbook of Organic Conductive Molecules and Polymers, Vol. 4, Wiley, Chichester, UK, 1997, p. 595.

[3] W.R. Cieslak (Ed.), Selected Battery Topics, PV 98-15, The Electrochemical Society Proceedings Series, Pennington, NJ, 1998.

[4] A. Rudge, J. Davey, I. Raistrick, S. Gottesfeld, J. Power Sources 47 (1994) 89.

[5] A. Rudge, I. Raistrick, S. Gottesfeld, J.P. Ferraris, Electrochim. Acta 39 (2) (1994) 273.

[6] C. Arribus, D. Rueda, Synth. Met. 79 (1996) 23.

[7] F. Fusalba, P. Gouerec, D. Villers, D. Belanger, J. Elect. Soc. 148 (1) (2001) A1–A6.

[8] J.P. Ferraris, M.M. Eissa, I.D. Brotherston, D.C. Loveday, A.A. Moxey, J. Elect. Chem. 489 (1998) 57.